Silicon enhances the growth of *Phaeodactylum tricornutum* Bohlin under green light and low temperature

Peipei Zhao[1,2]*, Wenhui Gu[1,2]*, Songcui Wu[1,2], Aiyou Huang[1], Linwen He[1], Xiujun Xie[3], Shan Gao[1,2], Baoyu Zhang[1], Jianfeng Niu[1], A. Peng Lin[1] & Guangce Wang[1]

[1]Institute of Oceanology, Chinese Academy of Sciences, Qingdao 266071, China, [2]College of Earth Sciences, University of Chinese Academy of Sciences, Beijing 100049, China, [3]College of Marine Science and Engineering, Tianjin University of Science & Technology, Tianjin 300457, China.

Phaeodactylum tricornutum Bohlin is an ideal model diatom; its complete genome is known, and it is an important economic microalgae. Although silicon is not required in laboratory and factory culture of this species, previous studies have shown that silicon starvation can lead to differential expression of miRNAs. The role that silicon plays in *P. tricornutum* growth in nature is poorly understood. In this study, we compared the growth rate of silicon starved *P. tricornutum* with that of normal cultured cells under different culture conditions. Pigment analysis, photosynthesis measurement, lipid analysis, and proteomic analysis showed that silicon plays an important role in *P. tricornutum* growth and that its presence allows the organism to grow well under green light and low temperature.

D iatoms, which play a vital role in the biogeochemical cycle, are responsible for one-fifth of the primary productivity on Earth[1–3]. This phylogenetically young group includes two major classes, the pennates and the centrics, and they are widespread in all kinds of aquatic environments[4]. The activity of diatoms dominates silicon cycling in the ocean[5,6]. For most diatoms, silicic acid greatly influences cell cycle progression, and they will stop at the G1/S or G2/M transition if the silicon supply is deficient[7,8]. It has been suggested that biogenic silica is an effective pH buffer that facilitates the enzymatic conversion of bicarbonate to dissolved CO_2, thus improving the efficiency of photosynthesis in diatoms[9]. Consequently, silicon plays a crucial role in the growth of diatoms.

Phaeodactylum tricornutum Bohlin is the first pennate diatom for which the complete genome is known[10]. It has three convertible morphotypes: oval, fusiform, and triradiate[11]. Its outer shell is weakly silicified, and silicification is restricted to one valve of the oval cells[12,13]. In a specific *P. tricornutum* accession, the most frequent morphotype is usually fusiform or triradiate, whereas the concentration of oval cells is very low. However, fusiform and triradiate cells can transform into oval forms under unfavorable growth conditions[13]. *P. tricornutum* is widespread in both coastal and inland waters, usually in unstable environments, including estuaries and rock pools[13,14]. Temperature, light quality, and salinity change rapidly in these environments[15], and the living environment in surface water greatly differs from that of bottom water. De Martino et al. (2011) proposed that different shapes of *P. tricornutum* are more prevalent under different culture conditions. For example, oval cells are better acclimated to benthic environments, as they have higher sedimentation rates and can adhere and glide on surfaces, whereas fusiform and triradiate cells are better acclimated to planktonic environments[16]. Oval cells also are better able to survive under stressed conditions (e.g., limited nutrients) and can convert to fusiform or triradiate cells under favorable conditions. Thus, it seems that conversion of the three morphotypes of *P. tricornutum* occurs when environmental factors change, and the requirement of silicon for the growth of *P. tricornutum* is probably correlated with environment conditions.

In laboratory culture, the habitat is stable and conditions usually are optimal, which differs significantly from the situation in the natural environment. Under laboratory conditions, silicon is not required for the growth of *P. tricornutum*[13], although all three morphotypes assimilate silicon[11,17–20]. Yang et al. (2013) reported that deprivation of silicon during *P. tricornutum* cultivation resulted in a better growth characteristics due to the omission of silicon induced cell breakage[21]. However, our previous study showed that miRNAs of silicon starved *P. tricornutum* were significantly different from those of the normal cultured cells[22]. As miRNAs are important post-transcriptional

regulators of gene expression in eukaryotes[23], these observed differences in miRNA demonstrate that silicon affects the physiological processes of *P. tricornutum*. However, silicon's role in *P. tricornutum* growth in nature is poorly understood.

In this study, we compared the growth rate of silicon starved *P. tricornutum* with that of normal cultured cells under different culture conditions. Pigment analysis, photosynthesis measurement, lipid analysis, and proteomic analysis were performed to evaluate the role that silicon plays in *P. tricornutum* growth.

Results

Growth of *P. tricornutum*. To study the role that silicon plays in the growth of *P. tricornutum*, culturing experiments were conducted. Figure 1a shows little difference between the growth curves of *P. tricornutum* under normal and silicon starved culture conditions. Figures 1b–h show the growth curves of normal cultured and silicon starved *P. tricornutum* when cultured under low salinity (salinity 20‰), high light (2000 μmol m^{-2} s^{-1}), different photoperiods, and different nutritional deficiencies (iron starvation or nitrogen starvation). Silicon did not influence the growth rate of *P. tricornutum* under any of these conditions.

Figure 2 shows the growth of cells cultured under different light qualities or low temperature (10°C). Silicon had no impact when *P. tricornutum* was cultured under red light (wavelength 647–700 nm) (Fig. 2a), whereas cells cultured under blue light (wavelength 470–475 nm) died after 3 days of culture (Fig. 2b). As 470–475 nm is located in the wave valley of the absorption spectra of chlorophyll *a*[24]. That is, the blue light cannot absorbed by chlorophyll *a*, that may be the reason for the death of the algae. Growth of normal cultured and silicon starved *P. tricornutum* differed when cultured under green light (wavelength 491–574 nm) and low temperature (Fig. 2c–e), as the cells grew more slowly when silicon was unavailable. These results show that silicon influences the growth of *P. tricornutum* under specific conditions, including low temperature and green light.

Pigment analysis. Under the normal culture condition, the concentrations of fucoxanthin and chlorophyll *a* were 11.88 ± 0.32 and 29.69 ± 1.47 (10^{-5} ng/cell) (Fig. 3a). When silicon was not available, the concentration of the two pigments decreased to 10.88 ± 0.13 and 24.71 ± 0.52 (10^{-5} ng/cell) after 48 h of cultivation. Thus, silicon influenced pigment biosynthesis or degradation in *P. tricornutum*.

Chlorophyll fluorescence measurements. Figure 3c show the effective quantum yields of PSII (Y(II)) and PSI (Y(I)) and the maximum quantum yield of PSII (F_v/F_m). Y(II) and Y(I) values did not differ significantly between normal cultured and silicon starved *P. tricornutum*, and the same was true for the electron transport rates of PSI (ETR(I)) and PSII (ETR(II)) (Fig. 3b). The F_v/F_m value of normal cultured *P. tricornutum* was 0.69 ± 0.016, whereas the value was 0.66 ± 0.007 after 48 h of silicon starvation. F_v/F_m reflects the maximum quantum yield of PSII and is a sensitive indicator of the photosynthetic performance of plants. It provides important information about the effect of environmental stress on the plant[25]. The decline in the F_v/F_m value shows that the lack of silicon decreased the antireversion force of *P. tricornutum*, but the lack of differences in the other photosynthesis data showed that it did not influence the photosynthetic efficiency during the experiment.

Lipid analysis. The incipient relative fluorescence intensity of Nile red stained *P. tricornutum* was 45.08 ± 0.85, and the value dropped to 16.95 ± 1.21 and 11.47 ± 0.36, respectively, after re-culture in sterilized artificial seawater with normal or silicon-free f/2 media for 48 h. Figure 4 shows *P. tricornutum* cells stained with Nile red. Nile red stained lipid bodies showed characteristic yellow fluorescence under the microscope, with no significant difference between the two type of cultured cells.

Table 1 shows the fatty acid composition of normal cultured and silicon starved *P. tricornutum*. Total saturated fatty acids and total unsaturated fatty acids of normal cultured *P. tricornutum* represented 13.95% and 61.89% of the fatty acid content, respectively. The amount of total saturated fatty acids increased to 15.07% and that of total unsaturated fatty acids dropped to 61.14% when the cells were starved of silicon for 48 h. These results indicate that silicon deficiency did not influence the lipid content but did influence the fatty acid composition of *P. tricornutum*.

Protein extraction. 2-DE analysis of the extracted total protein was conducted before LC–MS/MS was carried out to ensure that the protein was properly prepared for further analysis. In Fig. 5, the protein spots are clearly displayed. Analysis using PDQuest 2-D Analysis Software (Bio-Rad) identified 1,293 and 1,559 protein spots in normal cultured and silicon starved *P. tricornutum*, respectively. The 2-DE results indicated that there were no problems with these proteins, thus they were suitable for subsequent LC–MS/MS analysis.

Protein expression and identification by LC–MS/MS analysis. *LC–MS/MS analysis*. For LC–MS/MS, each sample was analyzed three times. The whole analysis yielded 374 positive identifications with a protein score exceeding 15. Among them, 33 were up-regulated and 37 were down-regulated in silicon starved cells. The proteins of interest are shown in Table 2. The potential cellular functions of all of the differentially expressed proteins identified were searched for in UniProt (http://www.uniprot.org/) (Table 2, Fig. 6). More than one-third of the proteins had no notation in the database. Other proteins were classed into categories such as carbon metabolism, lipid metabolism, protein synthesis, and photosynthesis. Below we describe our proteome results according to this classification.

Central carbon metabolism. The abundance of two proteins, fructose-1,6-bisphosphate aldolase precursor (UniProt Accession number Q84XB5) and fructose-bisphosphate aldolase (B7GE67), which are related to glycolysis, changed after 48 h silicon starvation. Expression of two proteins, acetyl-CoA carboxylase (B7G7S4) and long chain acyl-CoA synthetase (B7FYK0), which are involved in lipid synthesis, was up-regulated when silicon was unavailable. Acetyl-CoA carboxylase catalyzes the first reaction of the fatty acid biosynthetic pathway, which involves the formation of malonyl-CoA from acetyl-CoA and CO_2[26]. This reaction is a committed step in fatty acid synthesis, and the enzyme is key in regulating rates of fatty acid synthesis[27]. However, not all of the malonyl-CoA generated by acetyl-CoA carboxylase is a precursor for de novo fatty acid biosynthesis and elongation; some of it contributes to secondary metabolites, such as flavonoids, stilbenoids, malonic acid, and malonyl derivatives[28]. It is difficult to conclude that the up-regulation of acetyl-CoA carboxylase can directly lead to the accumulation of fatty acids.

Expression of two subunits (H1A8C7 and A0T0E2) of the key enzyme of the Calvin cycle, ribulose-1,5-bisphosphate carboxylase/oxygenase (Rubisco), was down-regulated when the cells were lack of silicon. Rubisco catalyzes the rate-limiting step of CO_2 fixation in photosynthesis. The large subunit of Rubisco contains the active site, whereas the small subunit is required for maximal catalysis and contributes to CO_2/O_2 specificity[29]. However, down-regulation of only one enzyme of the Calvin cycle may not influence CO_2 fixation and algal growth rate.

Photosynthesis and pigment biosynthesis. Several proteins, such as fucoxanthin chlorophyll *a/c* proteins (FCPs) (B7G871, etc.), were down-regulated after 48 h silicon starvation. FCPs are the antenna proteins of diatoms; they are homologs of the light-harvesting complexes (LHC) of higher plants. Down-regulation of FCPs might be
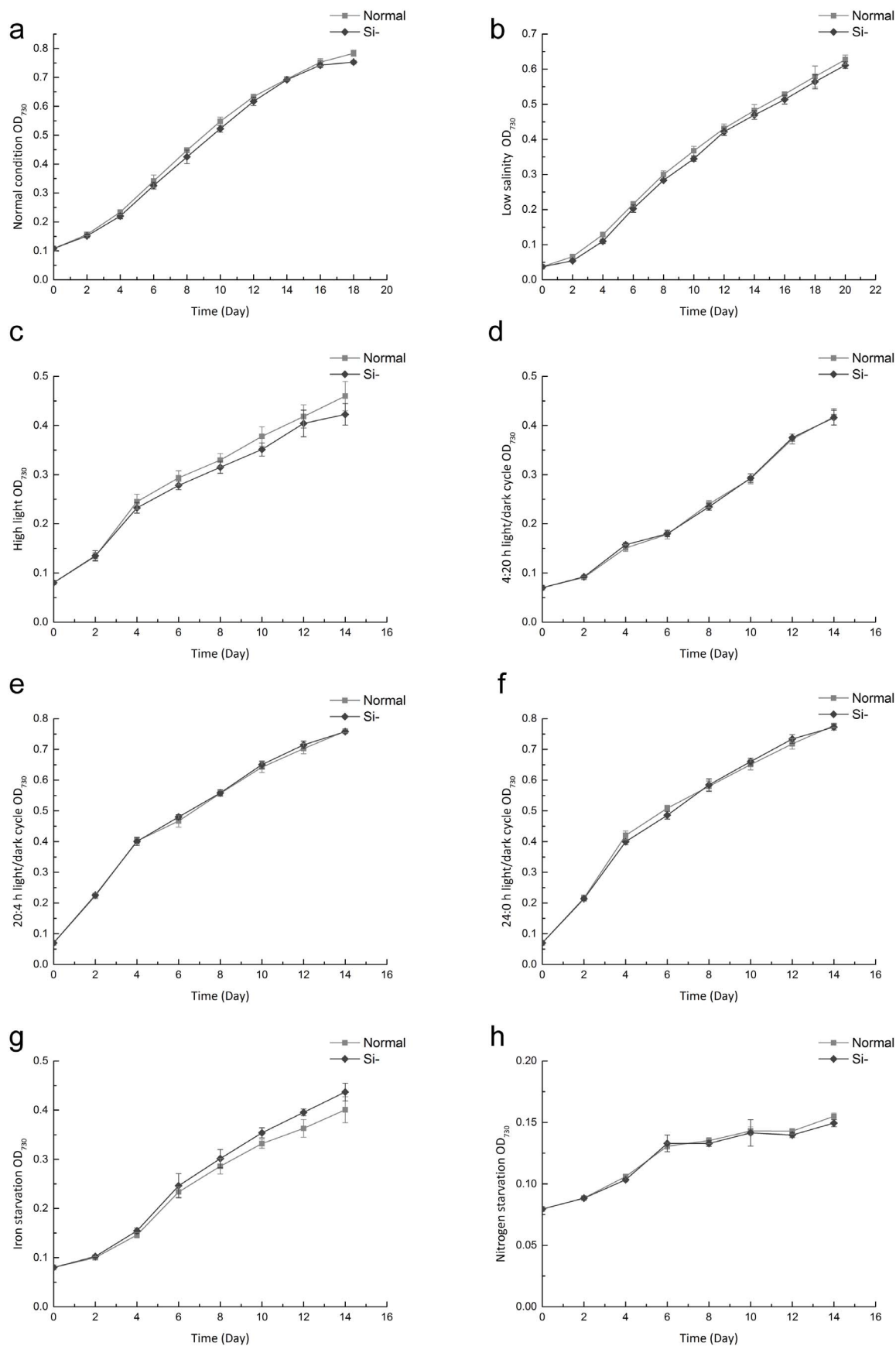
Figure 1 | Value of OD$_{730}$ of *P. tricornutum* under different culture conditions. (a) Normal (20°C, salinity 30‰, 24 μmol m^{-2} s^{-1}, and 12:12 h light/dark cycle). (b) Low salinity (salinity 20‰). (c) High light (2000 μmol m^{-2} s^{-1}). (d) 4:20 h light/dark cycle. (e) 20:4 h light/dark cycle. (f) 24:0 h light/dark cycle. (g) Iron starvation. (h) Nitrogen starvation. (Normal, normal cultured *P. tricornutum*. Si-, silicon starved cultured *P. tricornutum*.) The data are the mean of three independent experiments (±SD).
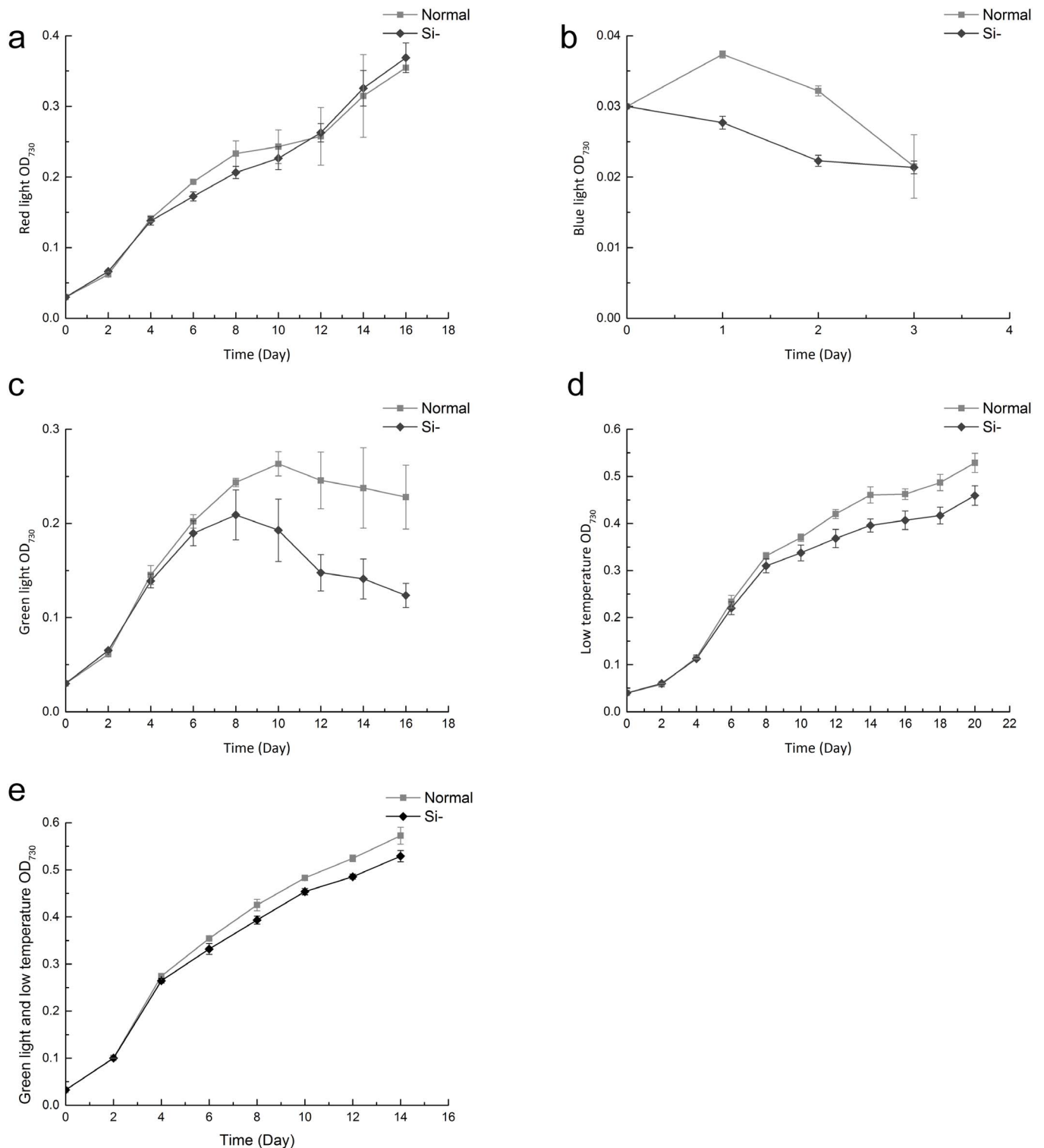
Figure 2 | Value of OD$_{730}$ of *P. tricornutum* under different culture conditions. (a) Red light (wavelength 647–700 nm). (b) Blue light (wavelength 470–475 nm). (c) Green light (wavelength 491–574 nm). (d) Low temperature (10°C). (e) Green light and low temperature. (Normal, normal cultured *P. tricornutum*. Si-, silicon starved cultured *P. tricornutum*.) The data are the mean of three independent experiments (±SD).
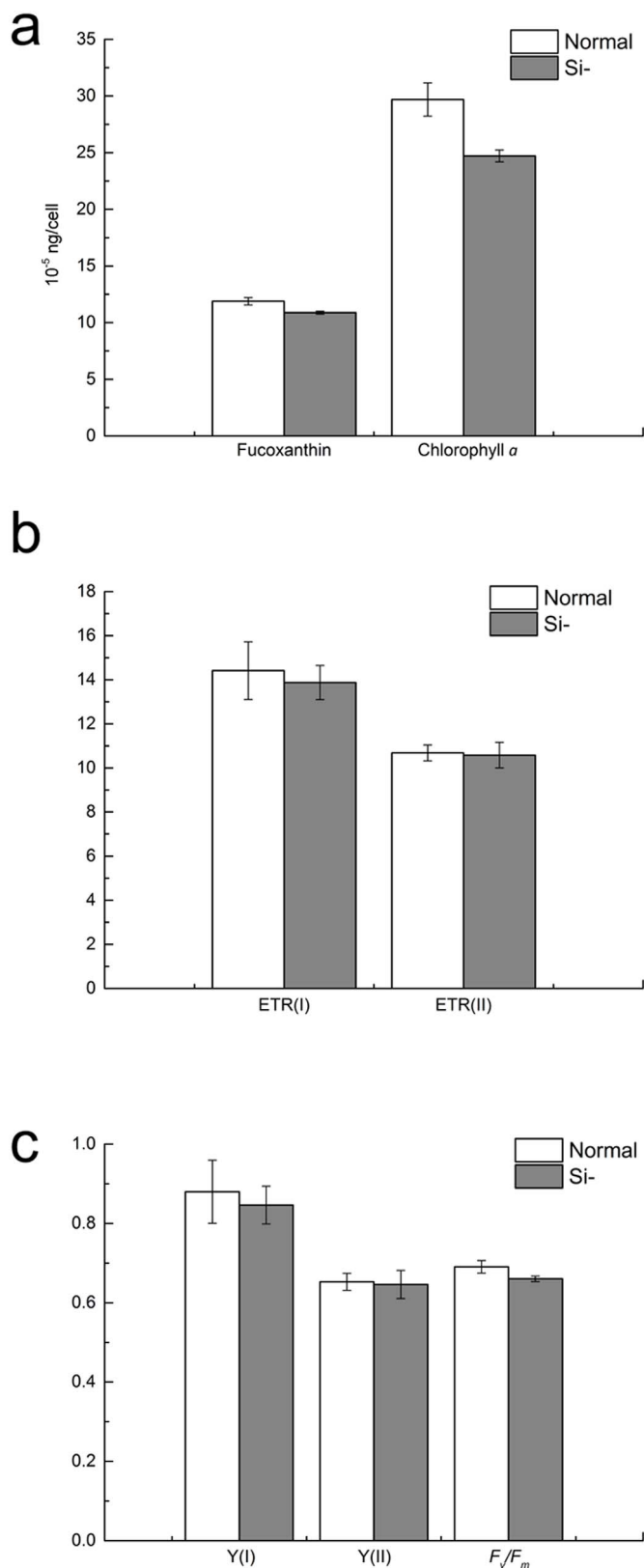
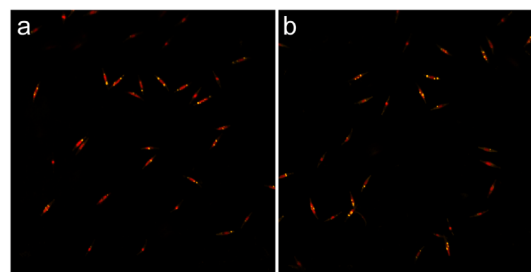accompanied by down-regulation of photosynthesis and photosynthetic pigment production.

The levels of a predicted protein (B7FP19) related to the chlorophyll biosynthetic process decreased when the silicon was unavailable. This indicates that the chlorophyll content may have decreased as well. Pigment analysis showed decreased levels of chlorophyll *a* and fucoxanthin, which was consistent with the proteome results. Photosynthesis analysis showed that the F_v/F_m value dropped,

whereas other photosynthesis data did not change, after 48 h of silicon starvation. As previously mentioned, lack of silicon decreased the antireversion force of *P. tricornutum*, but it did not appear to influence the photosynthetic efficiency.

Protein metabolism and chromosome integration. Expression of two translation elongation factors (B5Y4J2 and B8LEI9) was down-regulated when silicon was unavailable. Three predicted proteins

Figure 4 | *P. tricornutum* cells stained by Nile red. (a) Normal cultured *P. tricornutum*. (b) Silicon starved *P. tricornutum*.

(B7G715, B7FQU7, and B7G9G2) that function as structural constituents of ribosomes were regulated in two ways: two were up-regulated and one was down-regulated. A ubiquitin extension protein (B7FY02) was down-regulated. The proteome results suggested that protein synthesis declined and protein degradation increased when the cells were silicon starved. Three predicted proteins (B5YMD6, B7GB44, and B5Y3W7) for histone H3, nucleotide binding protein, and tubulin, respectively, were up-regulated when silicon was unavailable. The increased chromosome and cytoskeleton components suggested that chromatin tended to concentrate to the chromosome, prepared for a suitable condition for mitosis when the cells were lack of silicon.

Signal transduction. Expression of a polyubiquitin (Q1EFP9) and an annexin (B5Y5D4) was down-regulated when silicon was absent. Polyubiquitins are polymers formed through ubiquitin-ubiquitin conjugation, which usually occurs within cells and can be linked to target proteins[30]. Annexins are Ca^{2+} and phospholipid binding proteins, and they are present in both eukaryotes and prokaryotes[31]. Mortimer et al. (2008)[32] posited that annexins may be central regulators or effectors of plant growth and stress signaling. The decrease in stress tolerance associated proteins indicated that when the cells lacked silicon, their stress tolerance may have declined.

Figure 3 | Pigment contents and photosynthesis data of *P. tricornutum* under different culture conditions. (a) Fucoxanthin and chlorophyll *a* contents. (b) Electron transport rates of PSII (ETR(II)) and PSI (ETR(I)). (c) Effective quantum yields of PSII (Y(II)) and PSI (Y(I)), and maximum quantum yield of PSII (F_v/F_m). (Normal, normal cultured *P. tricornutum*. Si-, silicon starved cultured *P. tricornutum*.) The data are the mean of three independent experiments (±SD).

Table 1 | Fatty acid composition of *P. tricornutum* under different conditions. (Normal, normal cultured *P. tricornutum*. Si-, silicon starved *P. tricornutum*.)

NO.	Fatty Acids	Normal (%)	Si- (%)
1	14:00	4.97 ± 0.056	5.28 ± 0.044
2	15:00	0.14 ± 0.035	0.16 ± 0.020
3	16:00	8.44 ± 0.079	9.20 ± 0.21
4	16:1ω9	1.14 ± 0.020	0.79 ± 0.036
5	16:1ω7	27.31 ± 0.41	23.90 ± 0.32
6	16:1ω5	0.091 ± 0.006	0.08 ± 0.005
7	16:2ω4	4.18 ± 0.079	5.10 ± 0.23
8	16:4ω3	0.28 ± 0.056	0.45 ± 0.020
9	18:00	0.30 ± 0.020	0.33 ± 0.026
10	18:1ω9	0.88 ± 0.043	0.73 ± 0.026
11	18:1ω7	0.50 ± 0.026	0.45 ± 0.036
12	18:2ω6	1.57 ± 0.056	1.80 ± 0.072
13	18:3ω3	0.45 ± 0.036	0.47 ± 0.036
14	18:4ω3	0.22 ± 0.026	0.20 ± 0.010
15	18:00	0.099 ± 0.013	0.096 ± 0.002
16	20:1ω7	0.03 ± 0.003	0.062 ± 0.009
17	20:2ω6	0.55 ± 0.017	0.86 ± 0.034
18	20:3ω6	0.06 ± 0.002	0.064 ± 0.005
19	20:4ω6	0.58 ± 0.010	0.67 ± 0.030
20	20:4ω3	0.23 ± 0.010	0.19 ± 0.020
21	20:5ω3EPA	22.99 ± 0.17	24.21 ± 0.30
22	25:5ω3	0.38 ± 0.017	0.48 ± 0.069
23	22:6ω3DHA	0.45 ± 0.017	0.63 ± 0.035
24	total saturated fatty acids	13.95 ± 0.10	15.07 ± 0.18
25	total unsaturated fatty acids	61.89 ± 0.079	61.14 ± 0.29
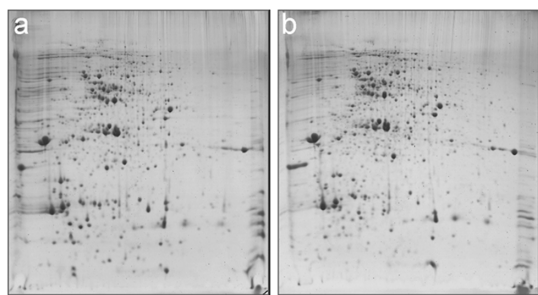
Figure 5 | Proteins separated (1.5 mg) by 2-DE (pI4-7). (a) Normal cultured *P. tricornutum*. (b) Silicon starved *P. tricornutum*.

Expression of a predicted protein (B7G386) with peroxidase activity and expression of a precursor of mutase superoxide dismutase (B7G0L6) were up-regulated when the cells were silicon starved. Peroxidase can respond to oxidative stress and superoxide dismutase catalyzes the dismutation of superoxide radicals[33]. As the content of fucoxanthin, an effective antioxidant[34], decreased when silicon was unavailable, the level of toxic reactive oxygen species (ROS) may have increased. Thus, the up-regulation of peroxidase and superoxide dismutase may have been a response to the increased level of ROS.

A predicted protein (B7G195) belonging to the small heat shock protein (HSP20) family was up-regulated after 48 h silicon starvation. HSPs can be induced by a wide variety of stressors, including elevated temperature. Expression of two predicted proteins (B7G4Y3 and B7G0Y4) that function as an intracellular protein transporter and an ammonium transmembrane transporter, respectively, was up-regulated when silicon was absent.

Analysis of mRNA expression. The mRNA expression levels of a randomly selected set of differentially expressed proteins in normal cultured and silicon starved *P. tricornutum* were measured by qRT-PCR using the RPS (ribosomal protein small subunit 30S) gene as an internal control. The RPS gene was stably expressed in *P. tricornutum*. The primer efficiencies of RPS, PFC (protein fucoxanthin chlorophyll *a/c* protein, B7G871), ANN (annexin, B5Y5D4), RBC (ribulose-1,5-bisphoaphate carboxylase/oxygenase small subunit, A0T0E2), and UBI (polyubiquitin, Q1EFP9) were 104.0, 105.0, 96.0, 100.9, and 103%, respectively. The level of ANN, RBC, and UBI expression in the normal cultured *P. tricornutum* was higher than that in the silicon starved cells (Fig. 7). This finding agrees with the proteome results, which showed a tendency for expression to decline at both the transcriptional and translational level when silicon was absent. The lack of a significant difference in PFC expression suggests that this gene may be post-transcriptionally controlled.

Discussion

The ocean is usually thought to be made of three principal layers, the surface layer is known as the mixed layer as much of the time it is mixed by currents, wind, and waves, and it is usually around 100–200 m thick[35]. However, the surface layer is not always well mixed, the very uppermost part of the surface layer is heated by the sun, the warm water floats on top, and there is a sharp transition to the cooler water below[35]. The temperature can change from about 25°C at the surface to below 10°C at the bottom of the layer, which differs in different latitudes. This phenomenon usually exists in the spring and summer in temperature and polar water, and the layer is called seasonal thermocline[35]. In clear ocean water blue light penetrates the deepest, secondly green light, for about 40–50 m, red light the least. However, coastal water often contains a lot of materials brought in by rivers that absorb blue light so that green penetrates deepest[35]. *P. tricornutum* can move vertically in the ocean, and it is widespread and occurs at different depths in the ocean. The oval cells are better acclimated to benthic environments, whereas fusiform and triradiate cells are better acclimated to planktonic environments[16]. The growth curves in the current study show that silicon influenced the growth rate of *P. tricornutum* only under conditions of low temperature and green light (Fig. 2); there was little difference under other conditions (Fig. 1). As temperature is lower in deep water and green and blue light are predominant, growth of *P. tricornutum* cells could be affected when they move to deep water. Lu et al. (2001) has reported that a high proportion of ovals was produced in fusiform trains under long-term stress of lower temperature[36]. Silicon starvation may interfere with the conversion from fusiform and triradiate cells to oval cells, which is the silicification valve-containing morphotype that is better acclimated to unfavorable growth conditions[13,36]. Thus, we suggest that silicon may affect the growth of *P. tricornutum* in deep water.

If the growth rate of *P. tricornutum* can be changed by silicon availability in deep water, the light-harvesting complex may be affected as well. As green and blue light are predominant in deep water, the corresponding photosynthetic pigment may be also influenced. Figure 3a and table 2 show that fucoxanthin and protein fucoxanthin chlorophyll *a/c* protein decreased as the cells were starved of silicon. The absorption maximum of fucoxanthin is near 490 nm. When it attaches to a protein in cells, the maximum is shifted by about 40 nm to longer wavelengths, thereby making available a larger fraction of the green light[37]. As fucoxanthin decreased when the cells were silicon starved, the absorption of green light decreased. The effective binding of fucoxanthin to the light-harvesting complex may also influence the absorption of light. If fucoxanthin cannot bind to the light-harvesting protein effectively when the cell is silicon starved, then photosynthesis efficiency as well as growth rate may decrease correspondingly. The growth curves under green light were consistent with the pigment and proteome results.

Fucoxanthin is an effective antioxidant[34], thus decreased fucoxanthin led to increased ROS. In response, expression of peroxidase and superoxide dismutase increased. Results of this study indicate that the gene for protein fucoxanthin chlorophyll *a/c* protein may be post-transcriptionally controlled, and our previous study of the specific expression of an miRNA targeting a protein fucoxanthin chl *a/c* protein under silicon starvation supports this premise[22].

Finley et al. (1987)[38] reported that the yeast polyubiquitin gene is essential for resistance to stresses such as high temperatures and starvation. One kind of polyubiquitin, called K63-linked chains, was reported to function in four pathways: the inflammatory response, DNA damage tolerance, ribosomal protein synthesis, and protein trafficking[30]. Another stress tolerance associated protein, annexin, has multiple functions, such as secretion, possible enzyme activity or interaction with other cellular proteins, interaction with actin, nucleotide phosphodiesterase activity, and acting as a substrate for protein phosphorylation, calcium channels, and peroxidases[39]. Annexins also may be central regulators or effectors of stress signaling and plant growth[32]. The decreased expression of two stress tolerance associated proteins in silicon starved *P. tricornutum* indicates that when the cells were starved of silicon, their stress tolerance may have declined.

Hazel (1995) reported that almost all poikilotherms increase the level of unsaturated fatty acids to maintain the appropriate fluidity of membrane lipids when the ambient temperature decreases[40], and Graham and Patterson (1982) found that the production of unsaturated fatty acids increases at low temperature in many plants[41]. Furthermore, cyanobacteria can enhance cold tolerance by increasing the amount of unsaturated fatty acids in genetically engineered membrane lipids as the cold-induced expression of genes for fatty acid desaturases increases[42]. Previous studies have shown that unsaturated fatty acids are important in maintenance of the photosystem II complex[42,43], particularly at low temperatures. Table 1 shows the observed changes in fatty acid composition and that total unsaturated fatty acids decreased when the cells were silicon starved. The decrease in total unsaturated fatty acids may influence the growth of *P. tricornu-*

Table 2 | Functional categories of selected proteins. (Differential expression proteins involved in carbon metabolism, pigment synthesis, photosynthesis and lipid metabolism in 48 h silicon starved *P. tricornutum* compared with that normal cultured. UniProt, Accession numbers from http://www.ebi.uniprot.org/index.shtml. Up/Down, Silicon starved *P. tricornutum* compared with normal cultured cells.)

| UniProt	Protein	Up/Down
Carbon Metabolism		
Q84XB5	Fructose-1,6-bisphosphate aldolase precursor	Down
B7GE67	Fructose-bisphosphate aldolase	Up
Lipid Metabolism		
B7G7S4	Acetyl-CoA carboxylase	Up
B7FYK0	Long chain acyl-CoA synthetase	Up
Calvin Cycle		
H1A8C7	Ribulose-1,5-bisphosphate carboxylase/oxygenase large subunit, partial (chloroplast)	Down
A0T0E2	Ribulose-1,5-bisphoaphate carboxylase/oxygenase small subunit	Down
Photosynthesis		
B7G871	Protein fucoxanthin chlorophyll *a/c* protein	Down
B7G5B6	Protein fucoxanthin chlorophyll *a/c* protein	Down
Q41093	Fucoxanthin-chlorophyll *a-c* binding protein E, chloroplastic	Down
B7G6Y1	Protein fucoxanthin chlorophyll *a/c* protein	Down
B7FZ94	Oxygen-evolving enhancer protein 3	Down
B7FR60	Protein fucoxanthin chlorophyll *a/c* protein	Up
Q8GTJ4	Fucoxanthin chlorophyll *a/c*-binding protein precursor	Down
B7GAS4	Protein fucoxanthin chl *a/c* protein	Down
B8C261	Fucoxanthin chlorophyll *a/c* protein 8	Down
B7G8E5	Fucoxanthin chlorophyll *a/c* protein, deviant	Down
Pigment Biosynthesis		
B7FP19	Predicted protein	Down
Cytoskeleton and chromosome		
B5YMD6	Predicted protein	Up
B7FX66	Histone linker H1	Down
B7GB44	Predicted protein	Up
B5Y3W7	Predicted protein	Up
Protein synthesis		
B5Y4J2	Translation elongation factor, EF-1, alpha subunit	Down
B7FY02	Ubiquitin extension protein 3	Up
B7G715	Predicted protein	Down
K0ST15	Hypothetical protein THAOC_10275	Down
B7FQU7	Predicted protein	Down
B8LEI9	Hypothetical protein THAPSDRAFT_bd1861	Down
B7G9G2	Predicted protein	Up
K0RCF5	Hypothetical protein THAOC_29407	Up
B7FWT8	Predicted protein	Up
Signal transduction		
B5Y5D4	Annexin	Down
Q1EFP9	Polyubiquitin	Down
B7FYL2	Iron starvation induced protein	Up
B7G386	Predicted protein	Up
B7GCM3	Flavodoxin	Up
B7G195	Predicted protein	Up
K0RB38	Hypothetical protein THAOC_35089, partial	Up
B7G0L6	Precursor of mutase superoxide dismutase [Fe/Mn]	Up
B7FYV4	Predicted protein	Up
B7G7G0	Predicted protein	Down
C7SYH8	Putative RNA-dependent RNA polymerase 2	Down
Transport		
B7G4Y3	Predicted protein	Up
B7G0Y4	Predicted protein	Up
Amino acid metabolism		
B7S466	Predicted protein	Down
B7FT14	Adenosylhomocysteinase	Down
B7GBF1	Predicted protein	Down

tum at low temperature by decreasing its tolerance to cold; that is, silicon may be beneficial for *P. tricornutum* living in deep water.

Methods

Strains and culture conditions. For the *P. tricornutum* culture, f/2 medium[44] made with steam-sterilized local seawater with f/2 vitamins (filter sterilized) and inorganic nutrients added was used. Cultures were incubated under cool-white fluorescent lights at 24 μmol m^{-2} s^{-1} on a 12:12 h light/dark cycle at 20°C for about 8 d and periodically stirred by hand. Cells were harvested by centrifugation for 5 min at

4,000 *g* and washed with sterilized artificial seawater[45]. Cells were re-cultured in normal or silicon-free f/2 media made with sterilized artificial seawater for 48 h. Cells were harvested by a two-step centrifugation process, initially at 4,000 *g* for 5 min and, after transfer to 1.5-mL Eppendorf tubes, 10,000 *g* for 2 min. Cell pellets were frozen instantly in liquid nitrogen and stored at −80°C before pigment extraction and protein extraction.

Growth measurement. Normal cultured cells and silicon starved cells for growth measurement experiments were cultured under conditions including low salinity (salinity 20‰), low temperature (10°C), different light quality (high light, red light,
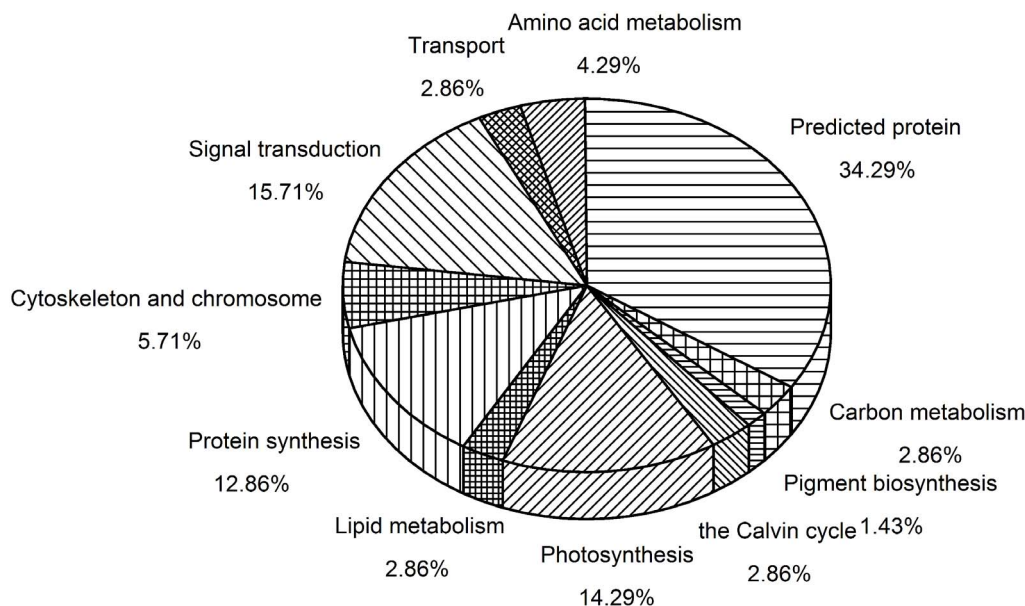
Figure 6 | Functional categories of differential expressed proteins separated by LC–MS/MS.

green light, and blue light), different photoperiod, and nutrient starvation (iron starvation, nitrogen starvation). The cell number was determined at a wave length of 730 nm using a UV-spectrophotometer (UV-1800, SHIMADZU, Japan) connected to a hemocytometer under an optical microscope (Nikon Eclipse E100, Japan).

Pigment analysis. The pigment extraction and HPLC analysis were carried out according to the method of Thayer and Björkman (1990), and Enriquez et al. (2010)[46,47] with some modifications. All procedures were carried out in dim light. The collected cells were suspended in acetone/methanol (1/1, v/v), placed in an ice bath for 30 min, and then centrifuged at 3,000 g for 5 min. The supernatant containing the pigments was collected and filtered through a 0.22 μm syringe filter. The filtered pigments were injected into an Agilent 1200 HPLC equipped with an Rx-C18 analytical column (4.6 × 250 mm) (Agilent Technologies Inc., Santa Clara, CA, USA). Analysis of the mobile phase, which consisted of water, methanol, acetonitrile, and ethyl acetate, was programmed as follows: 0–15 min, linear gradient from I (15% water, 30% methanol, 55% acetonitrile, 0% ethyl acetate) to II (0% water, 15% methanol, 85% acetonitrile, 0% ethyl acetate); 15–17 min, linear gradient from II to III (15% water, 15% methanol, 35% acetonitrile, 35% ethyl acetate); and 17–40 min, linear gradient from III to IV (0% water, 30% methanol, 0% acetonitrile, 70% ethyl acetate). The column temperature was 50°C and the flow rate was 0.75 mL/min. The pigments were detected by their absorbance at 443 nm.

Chlorophyll fluorescence and P700 measurement. Assessment of photosynthesis was carried out as described[48] with minor modification using a chlorophyll fluorometer Dual-PAM-100 (Heinz Walz GmbH, Germany). Briefly,samples of normal cultured cells and silicon starved cells were dark-adapted for 15 min before

the measurement. The induction curve was measured using the dual channel mode (Fluo + P700) with actinic light set at 24 μmol m^{-2} s^{-1}. The effective quantum yield and electron transport rate of both PS II and PS I (known as Y(II), Y(I), ETR(I) and ETR(II) respectively) and the maximum quantum yield of PS II (F_v/F_m) were calculated based on the data acquired during induction curve measurement.

Lipid analysis. Lipid content was determined by Nile red fluorescence staining following Liu et al. (2008)[49], the total lipids were extracted with chloroform/methanol (2/1, v/v), and the composition of fatty acids was quantified by gas chromatography[50]. That is, normal cultured cells and silicon starved cells were mixed with Nile red solution (0.1 mg mL^{-1} in acetone) (100/1, v/v), respectively, and settled for 7 min. Then the cells stained with Nile Red were analyzed on a fluorescence spectrophotometer (HITACHI F-4500, Tokyo, Japan) with 480 nm as the excitation wavelength and observed by Laser Confocal Microscopy, using a Carl Zeiss microscope with blue light as the excitation light.

Preparation of total protein. Cell pellets were ground in liquid nitrogen using a mortar and pestle with silica sand and polyvinyl-polypyrrolidone added. Pulverized cells were resuspended in 15 mL extraction buffer (5% w/v sodium dodecyl sulfate (SDS), 10% v/v glycerol, 5% v/v β-mercaptoethanol, 1% w/v complete protease inhibitor cocktail, 65 mM Tris-HCl pH 6.8) at 4°C for 1 h. The cell lysate was centrifuged at 8,000 g for 30 min at 4°C and the cell debris was removed. Proteins were precipitated overnight from the supernatant in 10% w/v trichloroacetic acid in 100% ice-cold acetone, centrifuged at 8,000 g for 30 min, rinsed three times in 100% ice-cold acetone, and rinsed once in 80% ice-cold acetone[51]. The pellet was air dried at 4°C.

Two-dimensional gel electrophoresis (2-DE) and image analysis. The protein was resolubilized in 100 μL of 0.2 M NaOH[52] and 2 mL of protein lysis buffer (7 M urea, 2 M thiourea, 4% w/v 3- [(3-cholamidopropy) dimethyl-ammonia]-1-propanesulfonate (CHAPS), 65 mM dithioethreitol (DTT)) overnight and then ultrafiltrated for 2 h. It was analyzed for total protein using bovine serum albumin as the standard[53]. A protein sample containing 1.5 mg of protein was mixed with 400 μL of solubilization buffer (7 M urea, 2 M thiourea, 4% w/v CHAPS, 65 mM DTT, 0.001% w/v bromochlorophenol blue, 0.2% w/v carrier ampholytes (Bio-lytes 3–10)). Immobilized pH gradient (IPG) strips (pI 4–7; 17 cm; Bio-Rad, Hercules, CA, USA) were rehydrated with the mixture at room temperature for 1 h then actively rehydrated at 50 V at 20°C for 18 h.

Isoelectric focusing (IEF) was performed at 20°C using the following parameters: linear 100 V for 1 h, 250 V for 1 h, 500 V for 1 h, a rapid increase from 500 V to 1,000 V for 1 h, a linear increase from 1,000 V to 8,000 V for 5 h, and then a hold at 8,000 V for a total of 60 kVh. After focusing, the IPG strips were equilibrated in 10 mL of equilibration buffer I (6 M urea, 2% w/v SDS, 20% v/v glycerol, 0.375 M Tris-HCl pH8.8, 65 mM DTT) followed by equilibration buffer II (6 M urea, 2% w/v SDS, 20% v/v glycerol, 0.375 M Tris-HCl pH8.8, 260 mM iodoacetamide) for 15 min each at room temperature. The gel strips were then washed in MilliQ water and equilibrated for 2 min in SDS-PAGE running buffer. The gel strip was positioned on top of a vertical 12% polyacrylamide gel, held in place by molten agarose (0.5% w/v agarose, 25 mM Tris, 192 mM glycine, 0.1% w/v SDS, 0.001% w/v bromochloro-phenol blue), and electrophoresed at a constant voltage of 80 V for 30 min and then 200 V for 8 h per gel. The gels were stained with blue silver[54], then scanned with
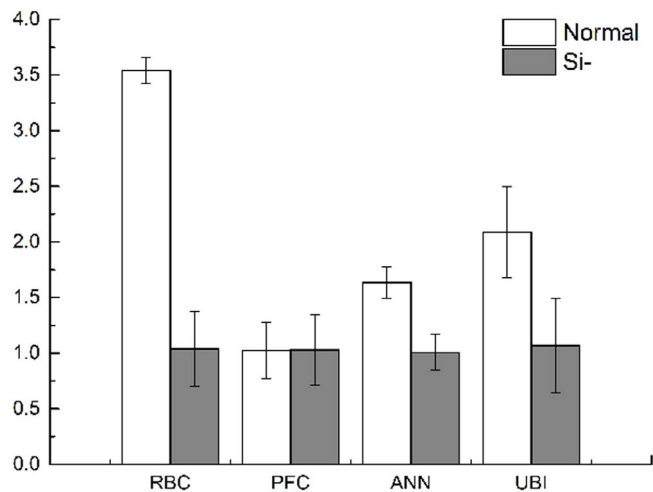
Figure 7 | Real-time fluorescent quantitative PCR (qPCR) of differential expressed proteins of normal and silicon starved *P. tricornutum.*

Table 3	Primers used in this study	
Name of genes	Sequence (5′-3′)
RPS (ribosomal protein small subunit 30S)	CGAAGTCAACCAGGAAACCAA GTGCAAGAGACCGGACATACC
PFC(protein fucoxanthin chlorophyll a/c protein)	GGCTACTTGGGAGACTTTGAC TGGCTATCGTGACGGAGGA
ANN (annexin)	CGGAACGAACGAAGCAGGAC ATGGGTTGGTAGCGAATCAGA
RBC(ribulose-1,5-bisphoaphate carboxylase/oxygenase small subunit)	ATGGGGTTTACCTTTATTTGATG AACGACCACCTTCTGGATTAGC
UBI (polyubiquitin)	CAGCCTTCGGATACTATTGACA AACGTGGGACTCCTTCTGGATG

Image Scanner (Bio-Rad GS-800). The images were analyzed using PDQuest 2-D Analysis Software (Bio-Rad).

Quantitative protein analysis by liquid chromatography/tandem mass spectrometry (LC-MS/MS). Protein solubilization was carried out as described[55]. Briefly, the protein was resolubilized in 8 M urea (125 mM NH_4HCO_3, pH 8) at 90°C for 20 min, cooled on ice, and quantified[53]. Protein was in-solution tryptic digested as previously described. The lysate was reduced by 10 mM DTT at 37°C for 1 h and then alkylated with 50 mM iodoacetamide for 30 min in the dark. Sequencing grade modified trypsin was used for in-solution digestion with trypsin/protein at 1/30. The peptides were acidified with 1% formic acid and stored at −80°C for LC-MS/MS analysis. The tryptic digested peptides were loaded onto a 2.1 mm × 150 mm reverse-phase column (Zorbax SB-C18, Agilent) connected to an Agilent 1200 HPLC system.

Peptides were eluted with gradient mobile phase solution A (0.1% formic acid in distilled water) and B (0.1% formic acid in acetonitrile) following Blonder et al. (2007)[56] with minor modifications. An acetonitrile gradient (3% B for 5 min, linear gradient from 3 to 50% B in 120 min; 95% B during 120 to 150 min) at a flow rate of 0.2 mL/min was used to elute the peptides into the Agilent 6520b Q-TOF mass spectrometer. The electrospray voltage used was 3.5 kV, and the drying gas temperature was set at 350°C. The fragmentor was set at 175 for ion transfer. Nitrogen gas was used during MS/MS analysis. Data acquisition was carried out in auto MS/MS mode using MassHunter software (version B03.01, Agilent).

All MS/MS spectra were processed using the Spectrum Mill MS Proteomics Workbench (version A.03.03, Agilent), and filtered MS/MS spectra data were searched against the NCBI diatom database (4/30/13 download) for protein identification. Precursor mass tolerance was set at ±20 ppm. One missed cleavage site was allowed during sequence matching. All protein identifications with a protein score ≥ 15 and a peptide scored peak intensity (SPI) ≥ 60% were considered as positive identifications. One shared peptides grouping method were used for protein rolling up. Finally, NCBI accession numbers were changed to UniProt numbers and searched through UniProt for molecular function, and cell location was summarized for the proteins in each sample.

Quantitative real time PCR (qRT-PCR) analysis. Total RNA was isolated using TRIZOL reagent (Gibco BRL, Grand Island, NY, USA), analyzed by agarose electrophoresis, and reverse-transcribed to cDNA. All procedures were carried out as described[57]. The transcript level of several differentially expressed proteins in normal cultured and silicon starved *P. tricornutum* was measured by qPCR using an iQ5 multicolor real time PCR detection system (Bio-Rad) in a total volume of 25 μL containing 12.5 μL of 2 × SYBR green master mix (Tiangen Biotech, Beijing, China), 2.5 μL (2 mM) of each primer, 2.5 μL of the diluted cDNA mix, and 5 μL of RNase-free water. The thermal profile for real time PCR was 95°C for 3 min followed by 35 cycles of 95°C for 15 s and 62°C for 30 s, followed by 72°C for 30 s. Dissociation curve analysis of the products was conducted at the end of each PCR reaction to confirm the presence of only one specific PCR amplification product. Triplicate qPCRs were performed for each sample, and the data were analyzed using the $2^{-\Delta\Delta Ct}$ method[58]. The primers used are shown in Table 3, and the RPS (ribosomal protein small subunit 30S) gene was used as the internal control[59].

Statistical analysis. All data shown are the mean ± standard deviation of results of three independent experiments. All statistical analyses were conducted using SPSS. One-way analysis of variance (ANOVA) was used to identify significant differences among groups. Differences were considered to be statistically significant at $P < 0.05$.

1. Field, C. B., Behrenfeld, M. J., Randerson, J. T. & Falkowski, P. Primary production of the biosphere: integrating terrestrial and oceanic components. *Science* **281**, 237–240 (1998).
2. Falkowski, P. G., Barber, R. T. & Smetacek, V. Biogeochemical controls and feedbacks on ocean primary production. *Science* **281**, 200–206 (1998).
3. Kroth, P. Molecular biology and the biotechnological potential of diatoms. *Adv. Exp. Med. Biol.* **616**, 23–33 (2007).
4. Norton, T. A., Melkonian, M. & Andersen, R. A. Algal biodiversity*. *Phycologia* **35**, 308–326 (1996).
5. Treguer, P. *et al.* The silica balance in the world ocean: a reestimate. *Science* **268**, 375–379 (1995).
6. Yool, A. & Tyrrell, T. Role of diatoms in regulating the ocean's silicon cycle. *Global Biogeochemical Cycles* **17**, 14–21 (2003).
7. Martin-Jézéquel, V. & Lopez, P. Silicon–a central metabolite for diatom growth and morphogenesis. *Progress in molecular and subcellular biology* **33**, 99 (2003).
8. Brzezinski, M., Olson, R. & Chisholm, S. Silicon availability and cell-cycle progression in marine diatoms. *Marine ecology progress series* **67**, 83–96 (1990).
9. Milligan, A. J. & Morel, F. M. A proton buffering role for silica in diatoms. *Science* **297**, 1848–1850 (2002).
10. Bowler, C. *et al.* The *Phaeodactylum* genome reveals the evolutionary history of diatom genomes. *Nature* **456**, 239–244 (2008).
11. Lewin, J. C., Lewin, R. & Philpott, D. Observations on *Phaeodactylum tricornutum*. *Journal of general microbiology* **18**, 418 (1958).
12. Borowitzka, M. A. & Volcani, B. E. The polymorphic diatom *Phaeodactylum tricornutum*: ultrastructure of its morphotypes. *Journal of Phycology* **14**, 10–21 (1978).
13. Martino, A. D. *et al.* Genetic and phenotypic characterization of *Phaeodactylum tricornutum* (Bacillariophyceae) accessions. *Journal of Phycology* **43**, 992–1009 (2007).
14. Rushforth, S. R., Johansen, J. R. & Sorensen, D. L. Occurrence of *Phaedcatylum tricornutum* in the great salt lake, Utah, USA. *Gt Basin Nat* **48**, 324–326 (1988).
15. Howland, R., Tappin, A., Uncles, R., Plummer, D. & Bloomer, N. Distributions and seasonal variability of pH and alkalinity in the Tweed Estuary, UK. *Science of the total environment* **251**, 125–138 (2000).
16. De Martino, A. *et al.* Physiological and molecular evidence that environmental changes elicit morphological interconversion in the model diatom *Phaeodactylum tricornutum*. *Protist* **162**, 462–481 (2011).
17. Thamatrakoln, K. & Hildebrand, M. Silicon uptake in diatoms revisited: a model for saturable and nonsaturable uptake kinetics and the role of silicon transporters. *Plant Physiology* **146**, 1397–1407 (2008).
18. Amo, Y. D. & Brzezinski, M. A. The chemical form of dissolved Si taken up by marine diatoms. *Journal of Phycology* **35**, 1162–1170 (1999).
19. Nelson, D. M., Riedel, G. F., Millan-Nunez, R. & Lara-Lara, J. R. Silicon uptake by algae with no known Si requirement. I. True cellular uptake and pH-induced precipitation by *Phaeodactylum tricornutum* (Bacillariophyceae) and *Platymonas* SP.(Prasinophyceae). *Journal of Phycology* **20**, 141–147 (1984).
20. Riedel, G. F. & Nelson, D. M. Silicon uptake by algae with no known Si requirement. II. Strong pH dependence of uptake kinetic parameters in *Phaeodactylum tricornutum* (Bacillariophyceae). *Journal of Phycology* **21**, 168–171 (1985).
21. Yang, Z. K. *et al.* Molecular and cellular mechanisms of neutral lipid accumulation in diatom following nitrogen deprivation. *Biotechnology for biofuels* **6**, 67 (2013).
22. Huang, A. Y., He, L. W. & Wang, G. C. Identification and characterization of microRNAs from *Phaeodactylum tricornutum* by high-throughput sequencing and bioinformatics analysis. *BMC Genomics* **12**, 337 (2011).
23. Lagos-Quintana, M., Rauhut, R., Lendeckel, W. & Tuschl, T. Identification of novel genes coding for small expressed RNAs. *Science* **294**, 853 (2001).
24. Björn, L. O., Papageorgiou, G. C. & Blankenship, R. E. A viewpoint: Why chlorophyll a? *Photosynthesis research* **99**, 85–98 (2009).
25. Maxwell, K. & Johnson, G. N. Chlorophyll fluorescence–a practical guide. *Journal of experimental botany* **51**, 659–668 (2000).
26. Ohlrogge, J. Lipid biosynthesis. *The Plant Cell* **7**, 957 (1995).
27. Hu, Q. *et al.* Microalgal triacylglycerols as feedstocks for biofuel production: perspectives and advances. *The Plant Journal* **54**, 621–639 (2008).
28. Nikolau, B. J., Ohlrogge, J. B. & Wurtele, E. S. Plant biotin-containing carboxylases. *Archives of Biochemistry and Biophysics* **414**, 211–222 (2003).
29. Spreitzer, R. J. Role of the small subunit in ribulose-1, 5-bisphosphate carboxylase/oxygenase. *Archives of biochemistry and biophysics* **414**, 141–149 (2003).
30. Pickart, C. M. & Fushman, D. Polyubiquitin chains: polymeric protein signals. *Current opinion in chemical biology* **8**, 610–616 (2004).
31. Gerke, V. & Moss, S. E. Annexins: from structure to function. *Physiological reviews* **82**, 331–371 (2002).
32. Mortimer, J. C. *et al.* Annexins: multifunctional components of growth and adaptation. *Journal of experimental botany* **59**, 533–544 (2008).
33. McCord, J. M. & Fridovich, I. Superoxide dismutase an enzymic function for erythrocuprein (hemocuprein). *Journal of Biological chemistry* **244**, 6049–6055 (1969).
34. Sangeetha, R., Bhaskar, N. & Baskaran, V. Comparative effects of β-carotene and fucoxanthin on retinol deficiency induced oxidative stress in rats. *Molecular and cellular biochemistry* **331**, 59–67 (2009).
35. Castro, P. & Huber, M. E. [Chemical and physical features of seawater and the world ocean] *Marine biology*. [Castro, P. & Huber, M. E. (ed.)] [48–50] (McGraw-Hill Higher Education, 2004).
36. Lu, K. H., Lin, X. & Qian, Y. X. Studies on the morphotype and morphological variation of *Phaeodactylum tricornutum*. *Journal of Ocean University of Qingdao* **31**, 61–68 (2001).
37. David , C. Fork. [Photosynthesis] *The science of photobiology*. [Smith, K. C. (ed.)] [336] (Plenum Publishing Corporation, New York, 1977).

38. Finley, D., Özkaynak, E. & Varshavsky, A. The yeast polyubiquitin gene is essential for resistance to high temperatures, starvation, and other stresses. *Cell* **48**, 1035–1046 (1987).

39. Delmer, D. & Potikha, T. Structures and functions of annexins in plants. *Cellular and molecular life sciences* **53**, 546–553 (1997).

40. Hazel, J. R. Thermal adaptation in biological membranes: is homeoviscous adaptation the explanation? *Annual Review of Physiology* **57**, 19–42 (1995).

41. Graham, D. & Patterson, B. D. Responses of plants to low, nonfreezing temperatures: proteins, metabolism, and acclimation. *Annual Review of Plant Physiology* **33**, 347–372 (1982).

42. Wada, H., Combos, Z. & Murata, N. Enhancement of chilling tolerance of a cyanobacterium by genetic manipulation of fatty acid desaturation. *Nature* **347**, 200–203 (1990).

43. Nishida, I. & Murata, N. Chilling sensitivity in plants and cyanobacteria: the crucial contribution of membrane lipids. *Annual review of plant biology* **47**, 541–568 (1996).

44. Guillard, R. R. L. [Culture of phytoplankton for feeding marine invertebrates] *Culture of marine invertebrate animals*. [Smith, W. L. & Chanley, M. H. (ed.)] [29–60] (Plenum Press, New York, 1975).

45. Harrison, P. J., Waters, R. E. & Taylor, F. A broad spectrum artificial sea water medium for coastal and open ocean phytoplankton. *Journal of Phycology* **16**, 28–35 (1980).

46. Enriquez, M. M. *et al.* Direct determination of the excited state energies of the xanthophylls diadinoxanthin and diatoxanthin from *Phaeodactylum tricornutum*. *Chemical Physics Letters* **493**, 353–357 (2010).

47. Thayer, S. S. & Björkman, O. Leaf xanthophyll content and composition in sun and shade determined by HPLC. *Photosynthesis Research* **23**, 331–343 (1990).

48. Gu, W. H. *et al.* Comparison of different cells of *Haematococcus pluvialis* reveals an extensive acclimation mechanism during its aging process: From a perspective of photosynthesis. *PloS one* **8**, e67028 (2013).

49. Liu, Z. Y., Wang, G. C. & Zhou, B. C. Effect of iron on growth and lipid accumulation in *Chlorella vulgaris*. *Bioresource Technology* **99**, 4717–4722 (2008).

50. Li, W. Q., Li, Q., Liao, Q. B. & Chen, Q. H. Effect of temperature on fatty acid composition of four species of microalgae. *Journal Of Oceanography In Taiwan Strait* **22**, 9–13 (2003).

51. Saravanan, R. S. & Rose, J. K. C. A critical evaluation of sample extraction techniques for enhanced proteomic analysis of recalcitrant plant tissues. *Proteomics* **4**, 2522–2532 (2004).

52. Nandakumar, M., Shen, J., Raman, B. & Marten, M. R. Solubilization of trichloroacetic acid (TCA) precipitated microbial proteins via NaOH for two-dimensional electrophoresis. *Journal of proteome research* **2**, 89–93 (2003).

53. Bradford, M. M. A rapid and sensitive method for the quantitation of microgram quantities of protein utilizing the principle of protein-dye binding. *Analytical biochemistry* **72**, 248–254 (1976).

54. Candiano, G. *et al.* Blue silver: a very sensitive colloidal Coomassie G-250 staining for proteome analysis. *Electrophoresis* **25**, 1327–1333 (2004).

55. Zhang, N. *et al.* Comparison of SDS-and methanol-assisted protein solubilization and digestion methods for *Escherichia coli* membrane proteome analysis by 2-D LC-MS/MS. *Proteomics* **7**, 484–493 (2007).

56. Blonder, J., Chan, K. C., Issaq, H. J. & Veenstra, T. D. Identification of membrane proteins from mammalian cell/tissue using methanol-facilitated solubilization and tryptic digestion coupled with 2D-LC-MS/MS. *Nature protocols* **1**, 2784–2790 (2007).

57. He, L. W., Zhang, X. J. & Wang, G. C. Expression analysis of phosphoenolpyruvate carboxykinase in *Porphyra haitanensis* (Rhodophyta) sporophytes and gametophytes. *Phycological Research* **61**, 172–179 (2013).

58. Livak, K. J. & Schmittgen, T. D. Analysis of relative gene expression data using real-time quantitative PCR and the $2^{-\Delta\Delta CT}$ method. *Methods* **25**, 402–408 (2001).

59. Siaut, M. *et al.* Molecular toolbox for studying diatom biology in *Phaeodactylum tricornutum*. *Gene* **406**, 23–35 (2007).

Acknowledgments

Author contributions

P.P.Z., W.H.G., S.C.W., L.W.H. and X.J.X. carried out the experiments. P.P.Z. and W.H.G. performed the data analysis. P.P.Z. drafted the manuscript. A.Y.H., S.G., B.Y.Z., J.F.N. and A.P.L. participated in data analysis. G.C.W. conceived of the study, and drafted the manuscript. All authors read and approved the final manuscript.

Additional information